Evolution of self-affine surface roughness in plastically deforming KCl single crystals

Edward M. Nadgorny[*]

The University of Edinburgh, Institute for Materials and Processes
The King's Buildings, Sanderson Building, Edinburgh EH93JL, UK
(on sabbatical leave from Michigan Technological University,
Physics Department, Houghton, MI, 49931, USA)
E-mail: nadgorny@mtu.edu

Jan Schwerdtfeger[1]**, Frederic Madani-Grasset**[1,2]**, Vasileios Koutsos**[1]**, Elias C. Aifantis**[2]**, and Michael Zaiser**[1]

[1] *The University of Edinburgh, Institute for Materials and Processes*
The King's Buildings, Sanderson Building, Edinburgh EH93JL, UK
[2] *Aristotle University of Thessaloniki, Polytechnic School, 54006 Thessaloniki, Greece*

We use scanning white-light interferometry to investigate the surface morphology evolution of KCl single crystals during plastic deformation in hardening stages I and II. We demonstrate that during deformation initially almost smooth as-cleaved surfaces develop self-affine roughness over several orders of magnitude in scale. The roughness exponent ζ of one-dimensional surface profiles is found to be close to 0.7. The kinetics of surface roughening is investigated, and the rate of roughening is shown to correlate with the hardening rate. During hardening stage II, a marked acceleration of the surface roughening rate is observed. The morphology of surface profiles changes at the transition between hardening stages I and II.

[*]Speaker.

1. Introduction

Plastic deformation leads to characteristic surface phenomena which can be used to monitor dislocation motions and gain information on plastic flow patterns. Surface micrographs have been used since the early fifties to characterize the arrangement and properties of slip lines in order to understand the underlying dislocation processes. More recently, *in situ* observation of the formation of slip lines and slip bands has provided information on the dynamic properties of dislocations and dislocation groups (for an overview, see the review by Neuhäuser [1]).

In recent years, there has been a renewed interest in surface investigations as a tool for monitoring the spatial organization of plastic deformation on multiple scales. Kleiser and Bocek [2], and Sprusil and Hnilica [3], analyzed the spatial arrangement of slip lines on deformed Cu and Cd single crystals in view of possible fractal patterns. Sprusil and Hnilica tried to deduce a fractal dimension by determining the mean slip line spacing from micrographs of different magnification, which is methodologically spurious as discussed in [4] in relation with the fractal analysis of dislocation cell patterns. Kleiser and Bocek [2], on the other hand, provided a systematic investigation using various techniques (gap width distribution, box counting, and correlation integral). They found that slip lines on the surface of a Cu single crystal that were generated within a narrow strain interval ($0.59 < \gamma < 0.69$) exhibit a statistically self-similar pattern over a range of scales between typically 0.06 and 2μm. The set of intersection points with a normal line was found to have a fractal dimension of $D \approx 0.4 - 0.7$, depending on the method of analysis used. Slip lines accumulating over a larger strain interval from the beginning of deformation, on the other hand, were shown to form a more or less homogeneous pattern without clear evidence of self-similar behavior.

Another method to obtain information about the large-scale organization of plastic flow is to look at the surface profile of the deformed crystal. In this manner, long-range correlations in the pattern of surface steps can be detected indirectly, even if the lateral resolution of the profiling technique is not sufficient to locate individual surface steps once deformation has progressed beyond the very first stages. The relation between one-dimensional surface profiles evolving from an initially smooth surface, and the surface strain, is straightforward: If we use a local coordinate system such that the x direction corresponds to the profile direction and the y direction is normal to the average direction of the deformed surface, and we assume deformation to occur by crystallographic slip on a single slip system, then for small deformations the derivative $y_x = \partial y/\partial x$ of the profile $y(x)$ is related to the shear strain γ on this slip system by

$$\partial y/\partial x = c(\gamma - \langle\gamma\rangle) =: \delta\gamma, \qquad (1.1)$$

where c is a geometrical factor that depends on the relative orientation of the surface with respect to the slip plane and the slip direction of the active slip system. The idea is then to investigate whether the surface develops self-affine roughness with a roughness exponent $\zeta > 0.5$. This implies long-range correlations of the generating process $\delta\gamma$ which decay like $\langle\delta\gamma(x)\delta\gamma(x')\rangle \propto |x-x'|^{2\zeta-2}$. This method was used by Zaiser and co-workers [5] to demonstrate long-range correlations in the plastic strain pattern of deformed Cu polycrystals. Using a combination of two experimental techniques – atomic force microscopy (AFM) and scanning white-light interferometry (SWLI) – self-affine scaling has been demonstrated over more than three orders of magnitude in scale, ranging from about 50 nm up to about 10^5 nm. The roughness exponent stabilized after an initial transient at

a strain-independent value of $\zeta \approx 0.75$, whereas the absolute magnitude of the surface roughness increased continually with increasing plastic strain.

In the investigation of Zaiser et. al. it remained unclear whether the observed upper limit of the self-affine scaling regime was related to the grain size of the polycrystalline aggregate or to the finite length of the analysed profiles. This point was clarified in an investigation of Wouters et. al. [6]. They investigated polycrystals of Al-Mg alloys with different grain sizes and demonstrated that the scaling regime is delimited by the grain size which acts as an intrinsic correlation length. The roughness exponents in their investigation, $\zeta \approx 0.85 - 0.9$, were somewhat higher than those reported by Zaiser et. al. [5]. Wouters et. al. also studied the growth of the absolute surface roughness (rms roughness) on scales above the correlation length and found this to increase approximately linearly with strain.

From the persistence of surface features during surface roughness growth and from the observed linear scaling of the rms roughness with strain, Wouters et. al. conclude that the roughening on scales above the grain size is essentially governed by differences in grain orientation and the resulting inhomogeneities of the deformation pattern on the grain scale. Zaiser et. al., on the other hand, interpret their observations in terms of intrinsic fluctuations of the deformation process within the grains, based on a theoretical model as described in [7, 8]. In view of these differences in interpretation, it is important to study the evolution of surface roughness in single crystals where grain size effects, either due to different grain orientation or due to grain boundaries acting as obstacles to correlated dislocation motion, can be ruled out. The present paper provides first results of such an investigation on KCl single crystals.

The crystals are of the rocksalt structure that consists of two interpenetrating f.c.c. lattices for each type of ions. The structure can also be characterized by {110} lattice planes alternately occupied by K and Cl ions, with neighboring ions mutually oriented along ⟨110⟩ directions. These planes act as the primary slip planes. Consequently, the primary slip system at low homologous temperatures is of type ⟨110⟩{110}, while ⟨110⟩{100} and ⟨110⟩{111} are secondary slip systems [9]. All six possible Burgers vectors are of the type $\vec{b} = a_0/2\langle 110 \rangle$ but, unlike f.c.c. metals with ⟨110⟩{111} glide systems, there is only one glide plane for each given Burgers vector, as shown in Fig. 1. Similar to the other rocksalt ionic crystals, KCl cleaves readily by a propagating crack on a {100} plane. This feature of KCl allows making use of cleavage to easily prepare specimens for [001] compression deformation. From the point of view of surface investigations, this is an obvious advantage since one obtains specimens with quite smooth and well-defined initial surfaces.

As seen from Figure 1, if such a specimen is deformed along the [001] direction, the four primary slip systems are equally stressed, and usually only one of them becomes the active primary slip system near the yield stress (In Figure 1, a specific primary slip system, [01-1](011), is shown as such an example.) Then the system [011](01-1) is called the orthogonal slip system, and typically such a system also becomes active but in other parts of specimen, either simultaneously with the primary system or later at higher deformation and stress. Finally, after further deformation, the two other slip systems, [10-1](101) and [101](10-1) in our example, called the oblique slip systems, also become active.

It is well known that the stress-strain diagrams of rocksalt single crystals oriented for single slip are similar to those for f.c.c. metal single crystals [9, 10]. After the yield stress, hardening stage I begins with a small almost constant hardening rate and after deformation of several % changes into
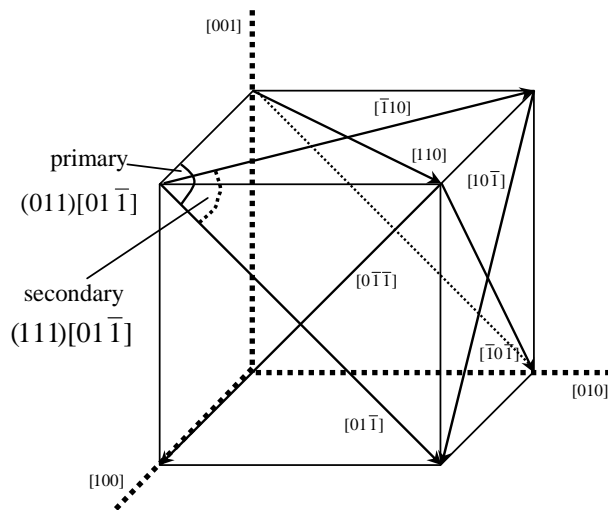
Figure 1: Geometry of dislocation glide in KCl single crystals. Six possible Burgers vectors of type $a_0/2\langle 110\rangle$ in six primary slip systems are shown. Also shown is one of the secondary slip systems.

Stage II with progressively increasing hardening rate. The dislocation structure developing above the yield stress is first characterized by several narrow slip lines in one of the primary glide systems. The slip lines then start spreading and convert into wider slip bands, and the other, orthogonal glide system also becomes active. As applied stress increases into Stage II, the structure becomes more complex, when oblique glide systems are also activated. Still, similarities with fcc crystals are found even at higher strains when complex cellular patterns may emerge which are reminiscent of those oberved in fcc single crystals deformed into hardening stage III [4].

2. Experimental

Rectangular specimens with { 100 } faces and dimensions of about 4x4x20 mm were prepared by cleavage from a large commercial "optical grade" single crystal. The specimens were deformed by compression in successive steps in a standard test machine, Instron 3360, at room temperature and at a crosshead rate of 0.002 mm/s corresponding to a nominal strain rate of 1×10^{-4} s^{-1}. Dislocation structures in as-cleaved specimens and after various deformation steps were revealed by selective etching and birefringence techniques. Chemical polishing was used to remove the dislocation etch pits before each following deformation step. Separate tests demonstrated that polishing has little influence on the deformation behavior: as-cleaved and polished specimens show very similar stress-strain diagrams including practically identical yield stresses. Some examples of evolving dislocation structures are shown in Figure 2 along the combined stress-strain diagram. As seen, there are dramatic changes in the dislocation density and structure after the yield point (compare the two left pictures), at the transition from Stage I into Stage II near 4 % strain, and during stage II (compare the two pictures taken at 3.8 % and 7.5 % strain shown with the same magnification). At deformation about 3%, the birefringence pattern also demonstrates at least two well developed active glide systems, the primary and oblique ones. Similar specimens and sequences of deformation steps were used for obtaining the surface profiles after each step. The
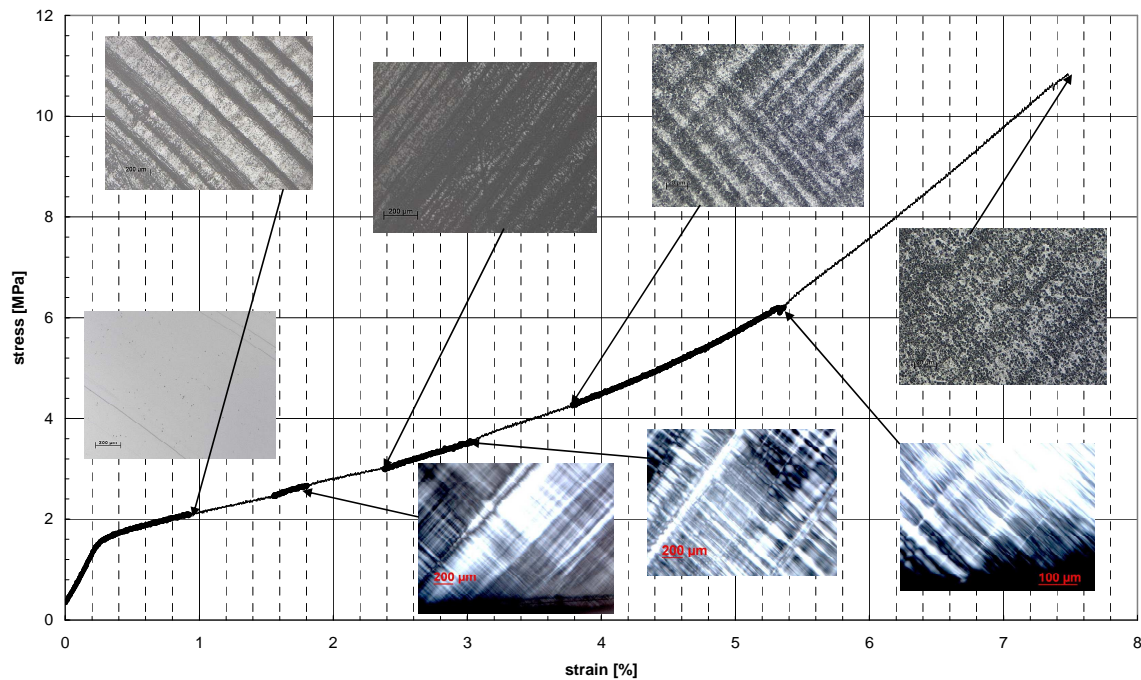
Figure 2: Combined normal stress-engineering strain curve of eight successive deformation steps of a KCl single crystal. The upper five pictures are obtained by selective etching (notice the ten-fold magnification increase in the pictures taken at 3.8 % and 7.5 % strain, indicating a much higher dislocation density in Stage II than in the first two pictures in Stage I). The lower three pictures are obtained by birefringence.

measurements were taken with a scanning white light interferometer (Zygo New View 100, of lateral resolution about 0.6 μm and vertical resolution 0.1 nm). After examining the as-cleaved specimen, two areas of 1700x130 μm were chosen on 100 cleavage terraces such that the initial surfaces were as smooth as possible, and their surface profiles were recorded. The compression then started in successive steps with the surfaces profiles measured after each deformation step on roughly the same areas. The area coordinates on the sample were fixed relatively to one of its corners allowing, in combination with topographical characteristics such as large cleavage steps, fairly precise location of the previously measured areas. At high deformation above about 7.5% engineering strain, the shape change of the specimen prevented further measurements with the necessary accuracy. From each area and for each deformation step, two 2D-profiles were extracted orthogonal to the slip lines.

3. Results

The deformation experiments on KCl reveal the typical three-stage hardening curve of alkali halide single crystals. Deformation at small strains (Stage I) proceeds in single slip with a comparatively low hardening rate, whereas at higher strains multiple slip systems become active and the strain hardening coefficient increases (Stage II, see Figures **??** and 3). Surface profiles were taken throughout these two hardening regimes using SWLI. At yet larger strains the hardening coefficient decreases again (Stage III); however, no surface investigations were carried out in this regime
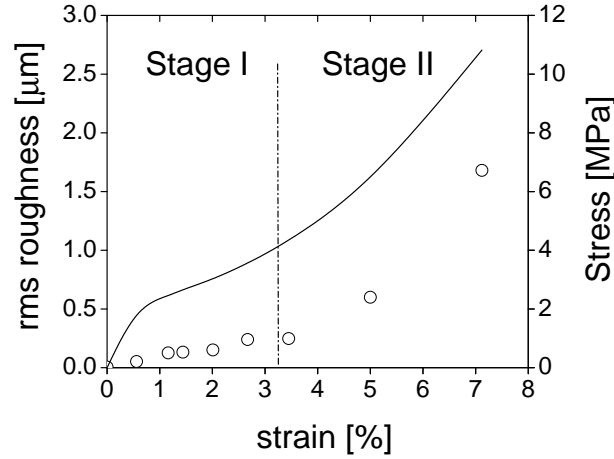
Figure 3: Stress-strain curve and rms surface roughness of a KCl single crystal deformed in compression at room temperature in [100] orientation; full line: stress-strain curve (compressive normal stress vs engineering strain), open circles: rms surface roughness as determined from 4 profiles with length 1.5 mm.

since the macroscopic shape distorsion of the compressed specimens became too large to permit a meaningful analysis of the surfaces.

All surface profiles were processed before analysis: (i) to remove effects of macroscopic surface curvature due to the shape distortion of the specimens during compression, 'trend curves' in the form of least-square fit fourth-order polynomials were subtracted from the $y(x)$ profiles. To check sensitivity of the procedure to the order of the fitting curve, analysis was also performed by fitting second and third-order polynomials. This has the effect that the overall roughness (root mean-square deviation of the entire profile) decreases slightly if the order of the 'trend curve' is increased. The roughness exponent was, however, little affected by such 'trend curve' changes.

Figure 3 shows the stress-strain curve together with the evolution of the rms surface roughness (root-mean-square deviation of the entire profile)

$$R_w = \left(\frac{1}{L} \int_L [y(x) - \langle y \rangle]^2 \mathrm{d}x \right)^{1/2} . \tag{3.1}$$

It is seen that the transition between hardening stages I and II corresponds to a marked increase in the rate of surface roughening. Whereas Wouters et. al. [6] in their experiments on Al-Mg polycrystals report an approximately linear increase of the overall surface roughness with strain, in KCl single crystals the increase is strongly nonlinear. The growth behavior can be described by an approximate growth exponent $\beta = \mathrm{d}\log R_w / \mathrm{d}\log \varepsilon \approx 0.8$ in stage I, and $\beta \approx 2.5$ in stage II.

To analyse the surface morphology, one-dimensional profiles were analyzed by evaluating the height difference correlation function $\langle y(x)y(x+l)\rangle$ as a function of the distance l along the profile. Also evaluated was the mean root-mean-square roughness of sub-profiles of length l,

$$R(l) = \left\langle \left(\frac{1}{l} \int_l [y(x) - \langle y \rangle]^2 \mathrm{d}x \right)^{1/2} \right\rangle , \tag{3.2}$$
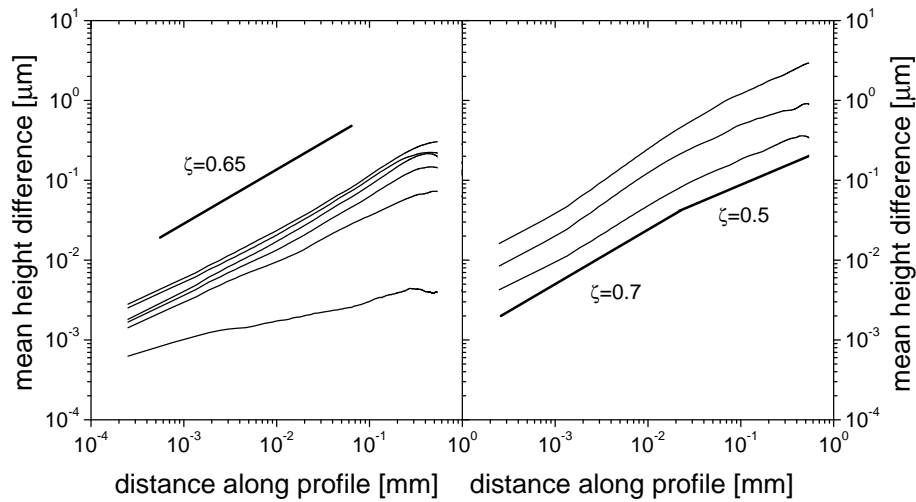
6

Figure 4: Local roughening of the surface of a KCl single crystal as determined by SWLI (mean height difference vs. distance along profile); left: deformation in Stage I; strains 0%, 0.56%, 1.16%, 1.44%, 2.01% and 2.67%; right: deformation in Stage II; strains 3.45%, 5.00% and 7.12%.

where the average runs over all sub-profiles of length l contained in the profiles ('variable-bandwidth method, [12]). For some profiles, also the Wavelet method as described by Nes et. al. [13] was applied for comparison.

The initial surface exhibits a quite small degree of roughness, with a value of $R_w < 10$ nm over a profile of 1 mm length. This mainly stems from mono-atomic surface steps created during cleavage; the distribution of these steps is irregular and gives rise to an initial roughness exponent $\zeta \approx 0.3$, a value which is atypical of fracture surfaces ($\zeta = 0.5 \ldots 0.8$). More investigations are, however, needed for characterizing the distribution of steps on the initial surface and firmly establishing this result.

During the very first stages of plastic deformation (up to an engineering strain of about 1%), the roughness exponent rises rapidly and R_w grows by one order of magnitude. The roughness exponent stabilizes then at a value $\zeta \approx 0.65 \ldots 0.7$ which remains constant throughout hardening Stage I, whereas the absolute height of the surface fluctuations continues to grow as discussed above. Throughout Stage I, no intrinsic limit exists to the self-affine scaling regime which extends over nearly 3 orders of magnitude and is limited only by the profile length (Figure 4, left).

At the transition to hardening stage II, at a strain of about 3.5%, the surface roughness growth rate increases significantly. At the same time, the morphology of the surface changes (Figure 4, right). In this regime, the profiles have a more complex structure, with a local roughness exponent $\zeta \approx 0.7 - 0.8$ on small scales which on larger scales possibly crosses over to an exponent of about $\zeta \approx 0.5$. The transition occurs at a characteristic length of about 30 μm; hence, the self-affine scaling regime is limited in this hardening stage.

To better understand the changes in profile morphology between Stage I and Stage II, it is instructive to look at a sequence of profiles taken at approximately the same location (Figure 5). During Stage I, the growth process is characterized by the stochastic accumulation of surface steps, and no persistent features can be detected on profiles taken at different strains (the first three graphs
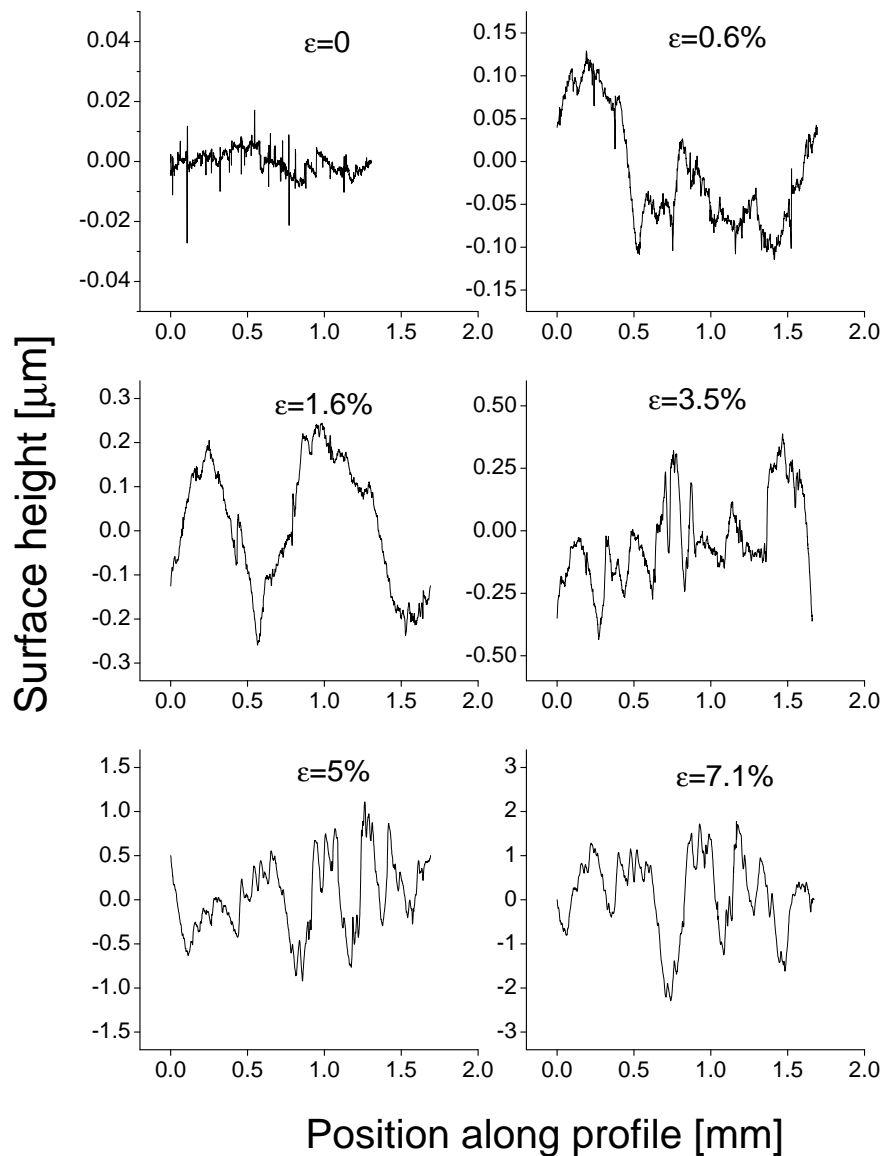
Figure 5: Evolution of surface roughness during deformation of a KCl single crystal: Profiles are taken from one location at different strains (horizontal axes: position along profile [mm], vertical axes: surface height [μm] (note the different scales on the different profiles). The transition between hardening stages I and II occurs at a strain of approximately 3%.

in Figure 5). This changes significantly in Stage II, where persistent features emerge on the profiles which grow in height but otherwise remain approximately unchanged (the second three graphs in Figure 5). These features can be interpreted as slip bands with a characteristic width of some 100 μm which roughly coincides with the upper end of the self-affine scaling regime. The persistence of these features over a strain interval of several percent indicates prolonged localization of slip in such bands during Stage II.

4. Discussion and Conclusions

Our investigation reveals two distinct regimes of surface roughening in hardening stages I and II, respectively. In stage I, deformation proceeds in single slip and roughening occurs through the stochastic accumulation of slip events (inside slip lines). The surface pattern is self-affine over three orders of magnitude in scale, and scaling is limited by only the finite length of the experimental profiles. The roughness exponent $\zeta \approx 0.7$ implies that the shear strain fluctuations $\delta\gamma = \gamma - \langle\gamma\rangle$ (γ is the shear strain on the active slip system) exhibit long-range correlations in this regime: The correlation function $\langle\delta\gamma(x)\delta\gamma(x')\rangle$ along the profile direction x decays as

$$\langle\delta\gamma(x)\delta\gamma(x')\rangle \propto |x-x'|^{2\zeta-2} \approx |x-x'|^{-0.6} \tag{4.1}$$

This finding is consistent with a fractal dimension of the slip-line pattern (pattern of intersection points of slip lines with the x direction) of around 0.4 as reported by Kleiser and Bocek [2] for deformation of Cu single crystals. It is also consistent with recent investigations of Weiss and Marsan [14] who report a fractal dimension of the three-dimensional pattern of slip events in deforming ice single crystals of about 2.5. All these data pertain to single slip deformation, albeit of different materials. This leads to the conclusion that data obtained by different experimental techniques, and from different materials, fit into a consistent picture according to which the spatial organization in single-glide deformation is characterized by random fractal patterns with a dimension around 0.5 (along a line drawn on the surface), 1.5 (on the surface) or 2.5 (in the bulk). The experimental roughness exponent of 0.7 is also in agreement with theoretical predictions obtained by Zaiser and co-workers [7, 8] from a stochastic continuum model of single-slip crystal plasticity.

The situation is more complicated in hardening stage II when multiple slip systems are active. There, the surface roughening process resembles much more the roughening observed in Al-Mg polycrystals as reported by Wouters et. al. [6]. Instead of a stochastic accumulation of slip events we observe the emergence of persistent features, which here can be interpreted as wide slip bands. This leads to an acceleration of roughness growth and an increase in the surface roughness exponent ζ. At the same time, a correlation length emerges which delimits the self-affine scaling regime from above. While all these features are similar to the observations in polycrystals, there are also important differences: The correlation length can not be related to any intrinsic material length scale (such as the grain size in the case of the polycrystal). The persistent features characterizing the roughness growth process are not associated with grown-in differences in material properties (grain orientation) but emerge spontaneously. Unfortunately the data in this regime are limited and larger strains are difficult to access because of the macroscopic shape distortion of the compression specimens. To better assess the evolution of surface morphology in Stage II, and the subsequent evolution into hardening stage III, we plan to conduct investigations analogous to the present one on Cu single crystals deformed in tension, where the problem of shape distortion is much less pronounced. In order to avoid not only the shape distortion but also multiple slip, we plan to partly irradiate KCl specimens to provide pure shear test conditions of single slip during Stage II as suggested by Smirnov [15].

The interpretation of surface observations of plastic flow always requires some caution in view of possible surface artefacts. The presence of a free surface modifies the stress field such that dislocations near surfaces experience image forces and may annihilate at the surface, leading to the

formation of a soft dislocation-depleted surface layer. Other effects are the preferential activation of sources near surfaces, and the fact that excess of dislocations of one sign near the surface may lead to local lattice curvature [16]. It is therefore important to combine surface and bulk observations in order to assess to which extent surface-based observations are representative of bulk behavior. For the KCl crystals investigated in the present study, such an investigation is under way in terms of characterizing the dislocation patterns near the surface (by etch pits) and in the bulk (by X-ray tomography). Results will be published in the near future. Regarding the present investigation of scale-invariant features on the surface, the mutual consistency between our results and the results by Weiss and Marsan regarding the bulk distribution of slip events gives some evidence that our results are indeed representative of bulk behavior.

For the investigation of scale-free patterns in plastic flow, surface-based techniques have one distinct advantage: Surface investigations give the possibility to characterize deformation-induced surface patterns from the atomic up to the macroscopic scale in terms of a single type of experimental information (surface height, positions of surface steps). Bulk techniques operating on different scales, by contrast, have to cope with the difficulty that the different techniques (e.g., transmission electron microscopy and X-ray topography) yield qualitatively different types of information. Data obtained by different techniques can therefore not be simply stitched together to yield a comprehensive picture. Surface techniques are therefore particularly suited to monitor the multiscale organization of plastic deformation through different stages of the deformation process and to detect scaling laws and scale-free features. To exploit this possiblility and assess the generality of the observations reported in this paper, we plan to extend our investigations to other types of materials. In particular, interesting questions arise in view of the behavior of materials which exhibit macroscopic plastic instabilities and coherent deformation modes (Lüders bands, PLC effect). This offers ample scope for continuing the present investigation in order to develop a comprehensive picture of surface morphology evolution during plastic deformation.

Acknowledgement

References

[1] H. Neuhäuser, *Slip-line formation and collective dislocation motion*, in: Dislocations in Solids, Vol. 6, edited by F.R.N. Nabarro (North-Holland, Amsterdam, 1983), p. 319.

[2] T. Kleiser and M. Bocek, *The fractal nature of slip in crystals*, Z. Metallkde. **77** (1986) 582.

[3] B. Sprusil and F. Hnilica, *Fractal character of slip lines of Cd single crystals*, Czech. J. Phys **35** (1985) 897.

[4] M. Zaiser, K. Bay and P. Hähner, *Fractal analysis of deformation-induced dislocation patterns*, Acta Mater. **49** (1999) 2463.

[5] M. Zaiser, F. Madani-Grasset, V. Koutsos and E.C. Aifantis, *Self-affine suface morphology of plastically deformed metals*, Phys. Rev. Letters **93** (2004) 195507.

[6] O. Wouters, J.P. Vellinga, J. Van Tijum and J.T.M. de Hosson, *On the evolution of surface roughness during deformation of polycrystalline aluminium alloys*, Acta Mater. **53** (2005) 4043.

[7] M. Zaiser and P. Moretti, *Fluctuation phenomena in crystal plasticity - a continuum model*, J. Stat. Mech, in press.

[8] M. Zaiser and E.C. Aifantis, *On the theory of gradient plasticity III: Random effects and slip avalanches*, Int. Journ. Plasticity, in press.

[9] M.T. Sparckling, *The Plastic Deformation of Simple Ionic Crystals* (Academic press, London, 1976).

[10] S.J. Basinski and Z.S. Basinski, *Work hardening*, in: Dislocations in Solids, Vol. 4, edited by F.R.N. Nabarro (North-Holland, Amsterdam, 1979), p. 261.

[11] M. Zaiser, S. Marras, E. Nadgorny, H. Strunk and E.C. Aifantis, *Fractal Dislocation Patterning in Plastically Deformed NaCl Polycrystals*, phys. stat. solidi (a) **185** (2001), R4-R7.

[12] J. Schmittbuhl, J. Vilotte, and S. Roux, *Reliability of self-affine measurements*, Phys. Rev. E **51** (1995) 131.

[13] I. Simonsen, A. Hansen, and O.M. Nes, *Determination of the Hurst exponent by use of wavelet transforms*, Phys. Rev. E **58** (1998) 2779 (1998).

[14] J.Weiss and D.Marsan, *Three-dimensional mapping of dislocation avalanches: clustering and space-time coupling*, Science **299** (2003), 89.

[15] B.I. Smirnov, Mechanical characteristics and the dislocation structure of LiF crystals deformed by slip along one system of crystallographic planes, Sov. Phys. Solid State **10** (1969) 2117.

[16] H. Mughrabi, *Some consequences of surface and size effects in plastically deformed copper single crystals*, phys. stat. sol. (b) **44** (1971) 391.